STUDY ON MULTIPLE MECHANISMS AND CONTRIBUTION WEIGHTS OF SLAGGING IN BIOMASS-FIRED BOILER

Yuting SUN[1], Jinyu SUN[2], Daoyang MA[2], Tongyu QIU[1], Yiming ZHU[1,*], Shunzhi YANG[3], Xuebin WANG[2]

[1]College of Energy and Environment, Liaoning Province Key Laboratory of Clean Energy, Shenyang Aerospace University, Shenyang, China

[2]MOE Key Laboratory of Thermo-Fluid Science and Engineering, Xi'an Jiaotong University, Xi'an, China

[3]Guoneng Xunxian Bio-Power Generation Co., Ltd., Hebi, China

*Corresponding author: zhuyiming16@126.com

To address the serious slagging issue in biomass boilers, field sampling, compositional analysis and corresponding FactSage thermodynamic calculations were conducted to study the slagging characteristics of a straw/bark-fired grate boiler. In addition to clarifying the multiple mechanisms, including the initial deposition by gaseous condensation and the fly ash capture by the viscous initial layer, the contribution weights of various mechanisms to the slagging behavior in four superheater areas were also obtained. Results indicate that K/Na double sulfates, rather than regular alkali sulfates, play a key role in forming the initial layer by condensation in high-temperature superheater. In 2nd mid-temperature superheater, the condensed KCl and less sulfate form high-viscosity initial layer, which captures fly ash easily and results in serious slagging. The composition evolution during slagging process simulated by FactSage indicates that low-temperature eutectics formed at high temperature area are more easily captured by the initial layer of high temperature superheater. The sulfates of K and Na start to combine below 950℃ and completely form $K_3Na(SO_4)_2$ at 750℃. K-Ca double sulfates exist above 850℃, while below 750℃ completely decompose into K_2SO_4 and $CaSO_4$. The gaseous condensation deposition contributes over 45% in the slagging of high/mid-temperature superheater, and only 8.4% in low-temperature superheater. The results provide a basis for the slagging prediction and prevention in biomass-fired grate boiler.

Key words*: Biomass-fired grate boiler, Slagging, Gaseous condensation, Viscous capture, Thermodynamic calculation,*

1. Introduction

Excessive emissions of CO_2 and global warming have become major issues affecting human survival and economic development. The Intergovernmental Panel on Climate Change (IPCC) pointed

out a demand of zero global CO_2 emissions by 2050 to ensure a temperature rise below 1.5℃ by 2100 [1].

The Chinese government has proposed a dual carbon target of peaking carbon emissions by 2030 and carbon neutrality by 2060 [2, 3]. The development of renewable energy has thus become the most prospective way [4, 5], and biomass energy has received extensive attention due to its excellent zero-carbon characteristics, especially in the field of replacing fossil energy combustion for power generation and heating [2]. Fluidized beds and grate boilers have become popular technologies for large-scale biomass combustion power generation [6]. However, biomass generally contains a large amount of alkali (earth) metal, which are prone to various serious ash-related problems such as slagging, corrosion, and ash deposition during combustion [7, 8]. This results in an increase in unplanned cleaning activities, damages heat exchange elements and leads to frequent shutdowns and unplanned repairs of the boiler [9].

A large number of relevant studies have presented slagging as a continuous process [10, 11]. The alkali metal species in the biomass fuel are released into the flue gas during combustion [12-14], and with the decrease of flue gas temperature the initial deposition is formed on the heating surface. The initial deposition layer is composed of low melting point inorganic components [10], which are often viscous, and thus capture subsequent fly ash containing Si and Al [15], resulting in further aggravation of slagging deposition. Niu et al. [7] summarized the main mechanisms as alkali-induced slagging and silicate-induced slagging. KCl is generally considered to be the main substance of alkali-induced slagging [16]. It has been found that the slagging on the side of the biomass circulating fluidized bed boiler and the wall of the superheater are mainly composed of submicron particles containing K and Cl [17]. Zhu et al. [18] performed a slagging field sampling of a biomass grate boiler, and found that the condensation of KCl played a leading role in mid-temperature superheater slagging. Gaseous KCl is sometimes sulfated by SO_3 in the environment [19]. Similarly, the condensation of sulfate will form a viscous initial layer, which will further cause the deterioration of slagging [12, 16, 20]. This situation often occurs on the heating surface with higher temperature [21]. Wang et al. [22] found that high concentrations of low-melting-point alkali metal compounds can significantly increase the viscosity of slagging and lead to more serious slagging. Wang et al. [23] simulated the deposition of KCl and SiO_2 particles at different addition ratios, and found that the deposition rate increased with the increase of KCl ratio, which proved that the capture behavior of fly ash by the viscous layer played an important role in the deposition process. Similar to biomass boilers, Jia et al. [24] found low melting point sulfates of K and Na in the slag of municipal solid waste incineration boilers. It is also reported that $CaSO_4$ was found in the bottom layer of the slagging on the surface of the grate of the waste incineration boiler, indicating that alkaline earth metals also contribute to the formation of the viscous initial layer [25]. The reports on Ca are mainly focused on the ash melting problem [26], and the effect of the gaseous release and condensation of Ca on the initial layer needs to be further explored. Wei et al. [27] carried out on-site slagging sampling on the superheater of a boiler burning high-alkali coal, and found that the slag was rich in alkali (earth) metals, showing an obvious layered structure, indicating the formation of the initial deposition layer and the subsequent enrichment of fly ash. Wang et al. [28] analyzed the slagging of a high-alkali coal-fired boiler, indicating that the deposition can be mainly divided into silicate and sulfate, with significantly different contents in each layer. It can be seen that the condensation deposition mechanism of alkali (earth) metals and the viscous capture mechanism of fly ash are universal in

various fuel systems of coal/biomass/solid waste, which constitute an important part of ash slagging on the heat exchange area of the boiler. However, previous studies have predominantly focused on the role of KCl and single-component sulfates (K_2SO_4, Na_2SO_4) in slagging formation, while insufficient attention has been paid to the effects of alkali/alkaline-earth metal double sulfates (K/Ca, K/Na double sulfates) and their phase transition mechanisms under temperature gradients.

In addition, in the previous discussions on the slagging mechanism, the important role of a certain slagging mechanism in specific situations is habitually highlighted, and the discussion on the contribution of various slagging mechanisms in different situations is insufficient. To further explore the causes of biomass slagging under different heating surface conditions, the slagging deposits produced in the operation of a biomass-fired grate boiler were sampled on site, and the slagging formation process and mechanism of four representative positions were discussed. In addition, based on the FactSage thermodynamic software, the slagging deposition process of different heating surfaces was calculated and simulated, and the evolution of slagging composition based on the influence of temperature was discussed. By calculating the mass ratio of different slagging risk components, the contribution distribution of gas phase condensation and viscous capture was discussed. This work aims to deepen the understanding of biomass slagging, and provide data and theoretical basis for slagging prediction and control.

2. Experiment

2.1. Experimental materials

Sampling experiments were carried out in a biomass grate boiler. In the superheater area, the flue gas passes in turn through the third stage superheater (S3), the fourth stage superheater (S4), the second stage superheater (S2) and the first stage superheater (S1). In order to study the slagging mechanism under different heating surface conditions, four kinds of slagging samples were obtained in S3 (#1, high- temperature superheater area), S4 (#2, high-temperature superheater area), S2 (#3, mid-temperature superheater area) and S1 (#4, low-temperature superheater area) according to the flue gas process. The schematics of the grate boiler, sampling position and samples are shown in fig. 1.

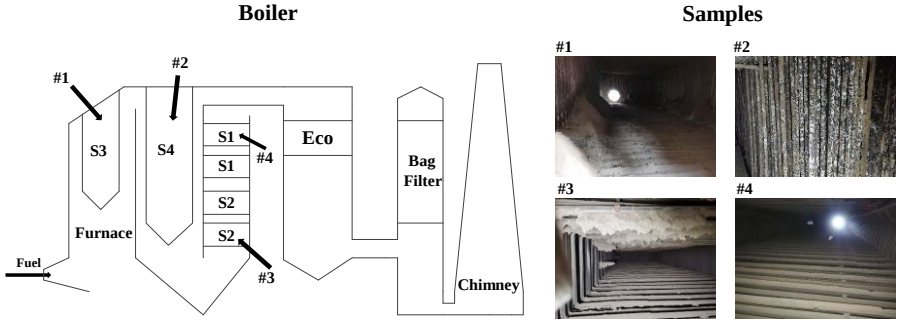

Fig. 1. Schematics of biomass-fired grate boiler, sampling position and samples

2.2. Experimental conditions and fuel analysis

During this experiment, the fuel used in the power plant was biomass fuel, composed of bark, capsicum annuum stalks, a small amount of wheat straw and construction waste wood.

The proximate analysis of the biomass fuel is carried out in accordance with the GBT28731-2012 standard. The results of proximate and ultimate analysis are shown in Table 1.

Table 1 Proximate and ultimate analysis of composite biomass fuel (unit: wt %)

Fuel	Proximate analysis				Ultimate analysis					
	M_{ad}	A_{ad}	V_{ad}	FC_{ad}	C_{ad}	H_{ad}	O_{ad}	N_{ad}	$St,_{ad}$	Cl_{ad}
Comprehensive material	2.48	4.05	72.14	21.35	45.62	5.66	41.3	0.78	0.14	0.33

The fuel was subjected to controlled incineration at 550℃. The composition of biomass ash produced by 550℃ incineration can reflect the mass of inorganic elements in the fuel [29]. The elementary composition of the biomass ash is shown in Table 2.

Table 2 The elementary composition of the biomass ash (ashing temperature: 550 ℃, unit: wt %)

Element	Si	Ca	K	Al	Mg	Na	Fe	S	Cl	O and others
Content	11.47	9.55	12.00	2.10	2.88	0.45	1.33	1.22	1.24	57.76

The flue gas temperature and wall temperature of the heating surface at each sampling location are shown in Table 3.

Table 3 Flue gas temperature and wall temperature

Position	Flue gas temperature/℃	Wall temperature/℃
Third stage superheater	950-1050	650
Fourth stage superheater	850-900	550
Second stage superheater	700	450
First stage superheater	510-600	300

2.3. Analysis apparatus

The slagging samples were further analyzed by X-ray diffraction (XRD) and X-ray fluorescence spectrometer (XRF). XRF is used for element determination of samples. The main crystalline phase components in the samples were determined by XRD, and the patterns were analyzed using Jade 6 software.

3. Thermodynamic calculation

FactSage7.2 software enables multi-conditional chemical equilibrium calculations. The Equilib module was used to calculate the equilibrium state of the main components in the superheater slagging, and the influence of temperature on the share (or transformation) of slagging components was obtained. The contribution of various slagging mechanisms in the slagging behavior of the superheater area was analyzed.

4. Result and discussion

4.1. Slagging characteristics of boiler superheater

4.1.1 High-temperature third stage superheater

The results of XRF analysis are shown in fig. 2 (a). The contents of K_2O, SO_3, SiO_2, CaO, and Cl account for 27%, 24%, 18%, 10% and 6%, respectively.

At high temperatures, volatile matter in biomass is released in the gaseous phase. K and Cl migrate with the flue gas and condense on heating surfaces to form a viscous layer, which serves as an important source of alkali metals in the deposits. During this process, S induces sulfation of alkali metal chlorides, converting them to sulfates [30], forming an initial deposition layer that captures large-particle fly ash dominated by Si.

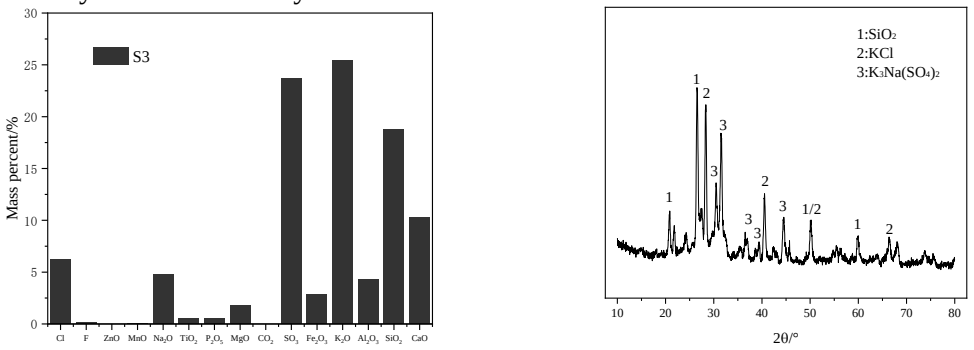

(a) XRF analysis of S3 sample **(b) XRD analysis of S3 sample**

Fig. 2. XRF and XRD analysis of S3 sample

As shown in fig. 2 (b), sharp KCl peaks were found in the XRD pattern. K_2SO_4 and Na_2SO_4 are not found. Instead, a significant amount of $K_3Na(SO_4)_2$ was identified, indicating that K and Na preferentially form double sulfates deposited on the wall surface, which combine with KCl to constitute the viscous initial deposition layer. The Si element in the slagging is almost entirely in the form of SiO_2.

The slagging mechanism in the third stage superheater area is primarily driven by condensed deposition layers formed from KCl and sulfate double salts, with viscous capture of fly ash serving as a secondary mechanism.

4.1.2 High-temperature fourth stage superheater

According to the XRF results in fig. 3 (a), in comparison with S3, the Cl content decreased by about 50%, and the contents of K, S, Si and Ca remained almost unchanged.

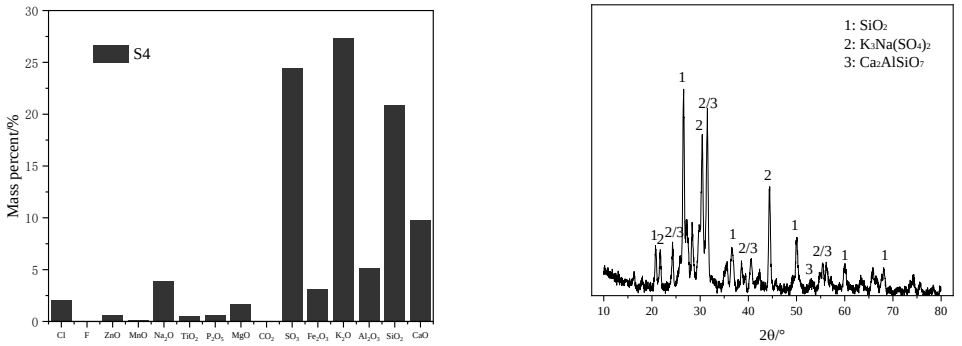

(a) XRF analysis of S4 sample **(b) XRD analysis of S4 sample**

Fig. 3. XRF and XRD analysis of S4 sample

Analysis of the XRD patterns in fig. 3 (b) reveals that the condensed deposition layer is almost entirely composed of $K_3Na(SO_4)_2$. In this region, the flue gas temperature ranges from 850-900℃, and the high S/Cl ratio significantly promotes sulfation processes [31]. The KCl in the flue gas and that condensed from the gaseous phase on the wall surfaces reacts almost completely with SO_3, forming a slag layer primarily composed of alkali metal sulfate double salts on the heating surfaces.The Si in the slagging of S4 is divided into two parts. One part remains as unreacted SiO_2, manifesting as refractory fly ash. The other portion of Si reacts with Ca in the flue gas to form Ca_2AlSiO_7 with a relatively low melting point, appearing as molten or semi-molten fly ash.

Sulfate has a higher melting point and lower viscosity than KCl. But when silicates are captured by the viscous layer, low-temperature eutectics or eutectic compounds form at the contact interfaces, resulting in increased viscosity of the slag layer. Concurrently, the thickening of fouling and deposition layers reduces the heat transfer efficiency of heating surfaces and elevates their temperature [32], which further promotes the melting of the viscous layer, and then increases the viscosity. The slagging mechanism at the S4 position is primarily dominated by gaseous condensation of alkali metal sulfate double salts, coupled with viscous capture of alkaline earth metal aluminosilicate melts and refractory fly ash.

4.1.3 Mid-temperature second stage superheater

The elemental composition of the slagging sample is shown in fig. 4 (a). Comparative analysis with high-temperature superheater sample reveals that the S2 slag exhibits a nearly 60% reduction in Si content, a significant 100%~300% increase in Cl content, while K and S levels remain largely unchanged.

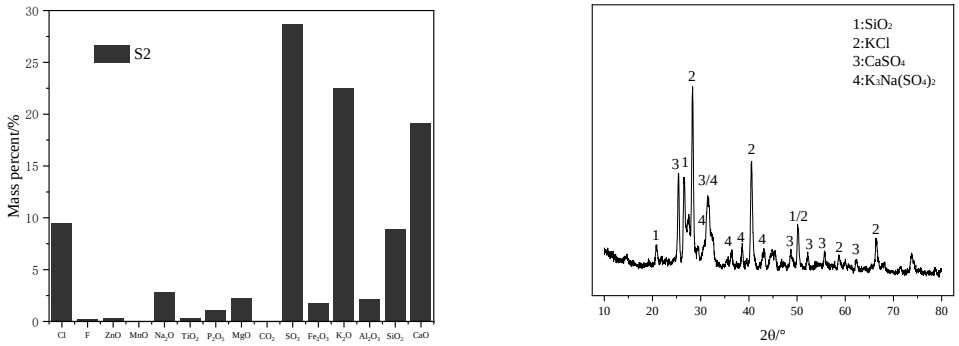

(a) XRF analysis of S2 sample **(b) XRD analysis of S2 sample**

Fig. 4. XRF and XRD analysis of S2 sample

The XRD result of the S2 slagging sample is shown in fig. 4 (b). Due to the temperature decrease, the sulfation of potassium KCl by S is significantly suppressed. A substantial amount of KCl undergoes gaseous condensation, becoming a major constituent of the condensation slag layer on the medium-temperature superheater surface. Partially sulfated K and Na retain strong chemical affinity, existing predominantly in the form of K-Na double sulfates. Due to the relatively low flue gas temperature in this area, $CaSO_4$ carried in the flue gas condenses into fly ash particles. These solidified $CaSO_4$ particles are subsequently captured via viscous capture mechanisms when transported by the flue gas to the initial slag layer.

On the contrary, ash deposition phenomena in the mid-temperature superheater area become more severe. According to previous reports, deposits on boiler heating surfaces exhibit a layered structure with " viscous layer-coarse particle layer-viscous layer " characteristics [7], indicating a coupling and mutually reinforcing relationship between the initial layer formed by gaseous condensation and the coarse slag layer. In this area with relatively low flue gas temperature, the coarse particles adhering to the viscous layers are composed of non-molten fly ash particles that lack viscosity, which to some extent promotes the growth of the condensed layer. Therefore, the condensation of gas phase salt at S2 is most obvious and the slagging is most serious. In summary, in the S2 area, the alkali metal, which is dominated by KCl and supplemented by sulfuric acid double salt, condenses to form a high-viscosity initial layer and viscous capture solid fly ash.

4.1.4 Low-temperature first stage superheater

The XRD and XRF analysis of the sample at S1 is shown in fig. 5 (a) and (b) respectively. It can be observed that the contents of Si and Ca are extremely high, with their oxides collectively approaching 60% of the total composition. The content of K, S and Cl decreased significantly, and the condensation of gaseous salt was not obvious.

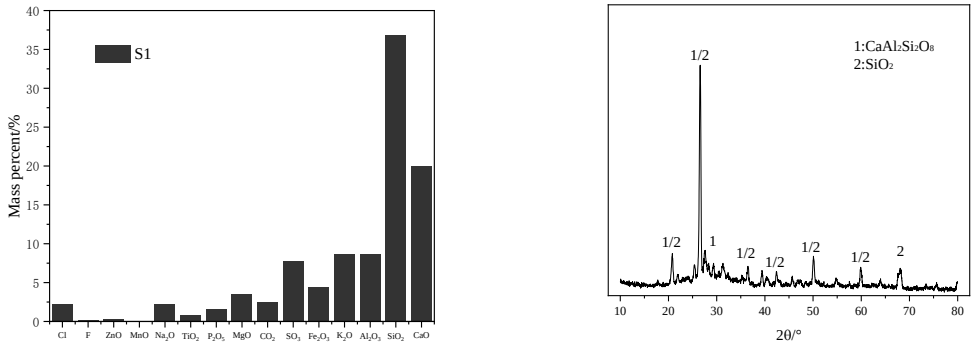

(a) XRF analysis of S1 sample **(b) XRD analysis of S1 sample**

Fig. 5. XRF and XRD analysis of S1 sample

XRD patterns reveal that the S1 slag samples predominantly consist of SiO_2 and $CaAl_2Si_2O_8$. In the vicinity of the S1 area, the content of alkali/alkaline earth metals is now minimal, allowing only limited formation of viscous layers. In this area with low flue gas velocity, fly ash particles entrained in the flue gas exhibit insufficient kinetic energy when approaching the initial slag layer, rendering them susceptible to capture and subsequent ash accumulation. The slagging mechanism here is that a small amount of ash particles with insufficient kinetic energy are adhered to the wall surface to form ash deposition.

4.2. FactSage thermodynamic calculation results and analysis

4.2.1 Thermodynamic equilibrium analysis

Based on the elemental composition of deposits on different heating surfaces described in Section 4.1 and the operating temperatures listed in Table 3, the ash deposition formation process on superheater heating surfaces during biomass fuel combustion was simulated using the Equilib thermodynamic calculation module in FactSage 7.2 software. The calculation takes 100 kg ash as the calculation reference, deduces the equilibrium process based on the influence of temperature, and discusses the possible chemical reactions. The calculation results are shown in fig. 6 (a)-(d).

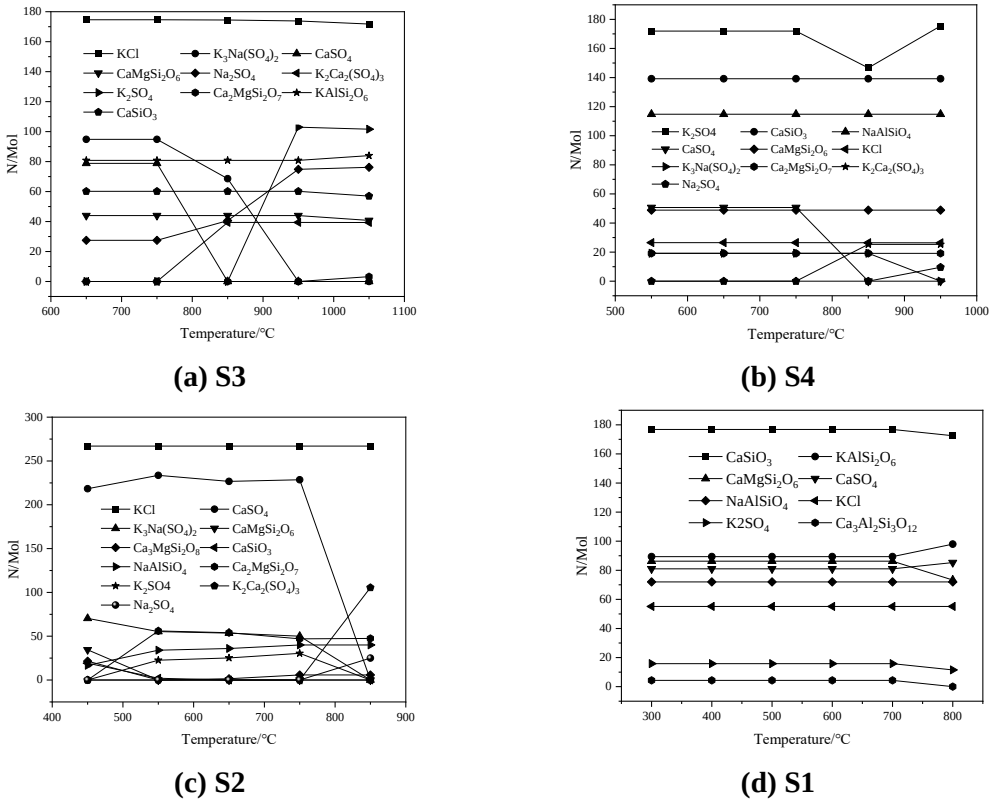

Fig. 6. The composition of slag on each heating surface varies with temperature

It can be observed that the deposits in the superheater are predominantly composed of KCl, sulfates, and silicates. Due to the difficulty of achieving complete reactions and thermodynamic equilibrium in practical combustion processes, SiO_2 is present in the actual deposits. The composition and content of sulfate vary greatly with temperature. It can be seen from the analysis that the sulfate of K and Na shows affinity below 950°C. The lower the temperature, the easier it is for K and Na to form double sulfate, and it completely exists in the form of K-Na double sulfates below 750°C. The sulfates of K and Ca are combined into K-Ca double sulfates above 750°C, and the reaction is complete above 850°C. The silicate is basically stable in the superheater temperature range, indicating that the reaction of forming the melt is basically completed in the high temperature zone of the furnace.

4.2.2 Mass distribution of gaseous condensation and viscous capture

Studying the contribution distribution of different slagging mechanisms on different superheater surfaces to the deposition behavior is of great significance for the prediction and prevention of ash deposition on the heating surface. Based on the thermodynamic equilibrium calculation results of FactSage, the mass ratio of substances corresponding to the wall temperature conditions of each superheater is obtained. The mass proportion of the material can be regarded as the contribution proportion of the corresponding slagging mechanism in the complete slagging deposition behavior. The calculation results are shown in fig. 7.

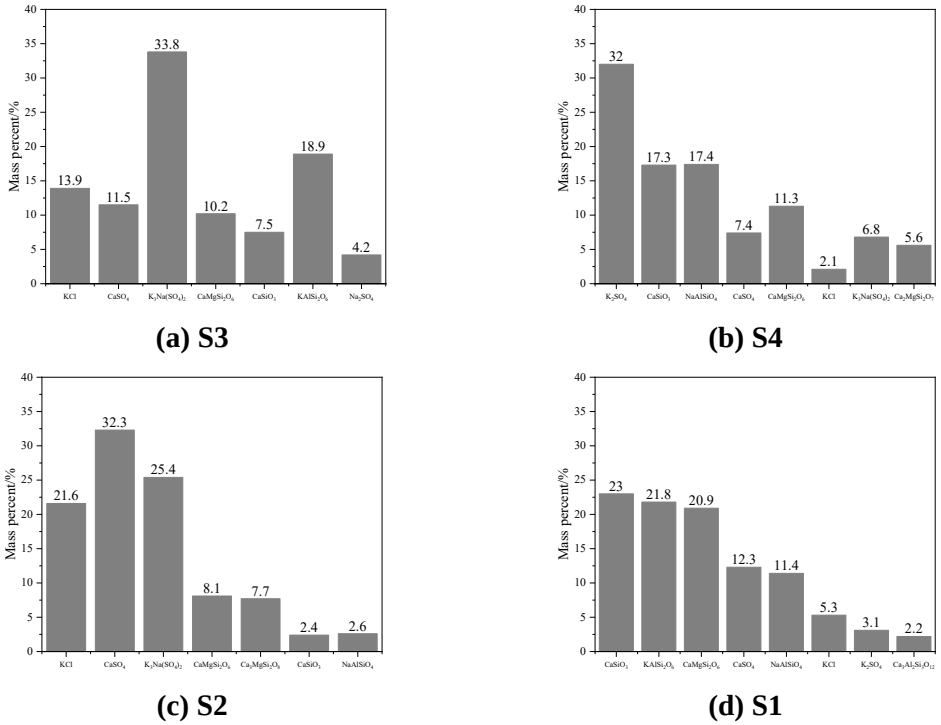

Fig. 7. Distribution of material mass ratio on superheater surface

Figs.7 (a)-(d) represent the mass ratios of each substance in the wall deposition of S3, S4, S2 and S1, respectively. In the calculation results, the silicon-containing substances can be regarded as large particles of ash in the flue gas captured by the initial viscous layer to the wall. Chlorides and sulfates of alkali metals can be considered as condensates constituting the initial viscous layer.

For S3 and S4, the temperature of flue gas flowing through high temperature overheating is higher, and the temperature of flue gas is often higher than 850℃. Combined with the research in Section 4.2.1, the source of $CaSO_4$ calculated under S3 and S4 wall temperature conditions is the low temperature decomposition of $K_2Ca_2(SO_4)_3$ condensate. $K_2Ca_2(SO_4)_3$ is micro acicular crystal on the surface of high temperature molten slag and increases the wall viscosity [33]. Therefore, the specific calculation method of the contribution of the slagging mechanism of high temperature superheater S3 and S4 is as follows:

$$R_{\text{condense}}=R_{\text{KCl}}+R_{\text{sulfates}} \quad (1)$$

$$R_{\text{all slagging}}=R_{\text{capture}}+R_{\text{condense}} \quad (2)$$

In the formula, R_{condense} represents the mass ratio of the viscous initial layer produced by the condensation of gaseous substances in the total slag/wt%. R_{KCl} represents the mass ratio of KCl/wt%. R_{sulfates} represent the mass ratio of sulfates (including alkali metals and alkaline earth metals)/wt%. R_{all} represents the sum of slag mass is 100%. R_{capture} represents the mass ratio of silicate/wt%. For S3, R_{condense}= 63.4%, R_{capture}= 36.6%. For S4, R_{condense}= 48.3%, R_{capture}= 51.7%.

For S2 and S1, the flue gas temperature flowing through the medium and low temperature superheater is reduced to below 700℃. At this time, the calculated $CaSO_4$ can only be used as the

solid fly ash formed by condensation in the flue gas, and it cannot be regarded as a component of the viscous layer. The specific calculation method for the slagging contribution of S2 and S1 is as follows:

$$R_{condense} = R_{KCl} + R_{sulfates\ of\ alkali} \quad (3)$$

$$R_{capture} = R_{silicates} + R_{CaSO_4} \quad (4)$$

$$R_{all\ slagging} = R_{capture} + R_{condense} \quad (5)$$

For S2, $R_{condense}$ = 47%, $R_{capture}$ = 53%. For S1, $R_{condense}$ = 8.4%, $R_{capture}$ = 91.6%.

The contribution of gas phase condensation deposition in the S3 region exceeds 60%. The S4 and S2 regions are easy to cause the condensation deposition of gas phase to produce a viscous layer, and the contribution to the viscous capture mechanism of fly ash increases to more than 50%, and the contribution of condensation deposition exceeds 45%. The phenomenon of gas phase condensation in the S1 region is not obvious, and more than 90% of the deposit comes from low kinetic energy fly ash which is easy to be captured by viscosity.

5. Conclusions

The slagging in the superheater area of straw/bark boiler is mainly caused by the initial deposition of gaseous condensation and the capture of fly ash by the viscous initial layer. K-Na double sulfate plays a key role in the formation of deposition layer in the high temperature superheater (S3, S4) area, and captures fly ash. The enriched KCl in the S2 region condenses with a small amount of sulfate to form a high-viscosity slagging layer, and the ability to viscously capture fly ash is strong. The gas phase condensation phenomenon in the S1 region is not obvious, and some fly ash with insufficient kinetic energy is captured by the wall surface, resulting in slight ash deposition.

Thermodynamic calculation results show that the formation of silicate mainly occurs in the high temperature furnace area, and the silicate in the superheater area shows a more stable melting/non-melting ash. The sulfate of K/Ca/Na is obviously affected by temperature during condensation. The sulfates of K and Na are stable sulfate monosulfates above 950℃. When the temperature is lower than 950℃, the sulfates of Na and K begin to combine, and Na_2SO_4 and K_2SO_4 are completely combined into $K_3Na(SO_4)_2$ below 750℃. The content of $K_2Ca_2(SO_4)_3$ is stable in the range of 850-950℃, and it is completely decomposed into K_2SO_4 and $CaSO_4$ below 750℃.

The contribution of the two slagging mechanisms to the slagging and fouling of the superheater was calculated. The gaseous condensation deposition contributes over 45% in the slagging of high/mid-temperature superheater, and only 8.4% in low-temperature superheater. The results provide a basis for the slagging prediction and prevention in biomass-fired grate boiler.

Acknowledgments

The authors gratefully acknowledge the support of the Natural Science Foundation of China (No.52106264), and the Science and Technology Plan Project of Liaoning Province, China (Special Project on Science and Technology Research) (no.2023JH1/10400006).

References

[1] Mikuli, H., et al., Flexible Carbon Capture and Utilization technologies in future energy systems and the utilization pathways of captured CO2, *Renewable and Sustainable Energy Reviews, 114*(2019), 109338
[2] Zhao, X., et al., Challenges toward carbon neutrality in China: Strategies and countermeasures, *Resources, Conservation and Recycling, 176*(2022), 105959
[3] Wang, J., et al., Does renewable energy technological innovation matter for green total factor productivity? Empirical evidence from Chinese provinces, *Sustain Energy Technol Assess, 55*(2023), 102996
[4] Ostergaard, P. A.,et al., Advances in renewable energy for sustainable development, *Renewable energy, 219*(2023), 119377
[5] Manzano-Agugliaro, F., et al., Scientific production of renewable energies worldwide: An overview, *Renewable & Sustainable Energy Reviews, 18*(2013), pp. 134-143
[6] Yin, C, Li S., Advancing grate-firing for greater environmental impacts and efficiency for decentralized biomass/wastes combustion, *Energy Procedia, 120*(2017), pp. 373-379
[7] Niu, Y., et al., Ash-related issues during biomass combustion: Alkali-induced slagging, silicate melt-induced slagging (ash fusion), agglomeration, corrosion, ash utilization, and related countermeasures, *Progress in Energy & Combustionence, 52*(2016), pp. 1-61
[8] Niu, Y., et al., Slagging Characteristics on the Superheaters of a 12 MW Biomass-Fired Boiler, *Energy Fuels, 24*(2010), pp. 5222-5227
[9] Khalil, R. A., et al., Experimental Investigation on Corrosion Abatement in Straw Combustion by Fuel Mixing, *Energy & Fuels, 26*(2014), 6, pp. 2687-2695
[10] Kleinhans, U., et al., Ash formation and deposition in coal and biomass fired combustion systems: Progress and challenges in the field of ash particle sticking and rebound behavior, *Progress in Energy and Combustion Science, 68*(2018), pp. 65-168
[11] Yongtie, C., et al., Modeling of ash formation and deposition processes in coal and biomass fired boilers: A comprehensive review, *Applied Energy, 230*(2018), pp. 1447-1544
[12] Wei, X., et al., Behaviour of gaseous chlorine and alkali metals during biomass thermal utilisation, *Fuel, 84*(2005), 7/8, pp. 841-848
[13] Johansen, J. M., et al., Release of K, Cl, and S during Pyrolysis and Combustion of High-Chlorine Biomass, *Energy & Fuels, 25*(2011), 11, pp. 4961-4971
[14] Wang, Z., et al., Alkali metal release in thermochemical conversion of biomass and coal: Optical measurements and modeling, *Progress in energy and combustion science, 100*(2024), 101131
[15] Yu, S., et al., Investigation on the influence of sulfur and chlorine on the initial deposition/fouling characteristics of a high-alkali coal, *Fuel Processing Technology, 198*(2020), 106234
[16] Garba, M. U., et al., Prediction of Potassium Chloride Sulfation and Its Effect on Deposition in Biomass-Fired Boilers, *Energy & Fuels, 26*(2012), 11, pp. 6501-6508
[17] Johansson, L. S., et al., Properties of Particles in the Fly Ash of a Biofuel-Fired Circulating Fluidized Bed (CFB) Boiler, *Energy & Fuels, 22*(2008), 5, pp. 3005-3015
[18] Zhu, Y. M., et al., Slagging characteristics in the superheater area and K/Ca distribution of biomass-fired grate boiler, *Sustainable Energy Technologies and Assessment, 59*(2023), 103403
[19] Hu, Z., et al., Emission characteristics of particulate matters from a 30 MW biomass-fired power plant in China, *Renewable Energy, 155*(2020), pp. 225-236

[20] Li, L., et al., Study on the Deposits Derived from a Biomass Circulating Fluidized-Bed Boiler, *Energy & Fuels,* 26(2012), 9, pp. 6008-6014
[21] Nutalapati, D., et al., Assessing slagging and fouling during biomass combustion: A thermodynamic approach allowing for alkali/ash reactions, *Fuel Processing Technology, 88*(2007), 11-12, pp. 1044-1052
[22] Wang, G., et al., Investigation on ash deposit formation during the co-firing of coal with agricultural residues in a large-scale laboratory furnace, *Fuel, 117*(2014), pp. 269-277
[23] Wang, Y., et al., Numerical investigation on deposition rate of mechanically mixed ash particles in an entrained flow reactor, *Asia-Pacific Journal of Chemical Engineering, 16*(2021), 5, e2685
[24] Jia, T., et al., Characteristics and mechanism of slagging in a 500t/d MSW incinerator, *Journal of the Energy Institute, 114*(2024), 101585
[25] Tang, Z., et al., Experimental investigation of ash deposits on convection heating surfaces of a circulating fluidized bed municipal solid waste incinerator, *Journal of Environmental Science, 48*(2016), pp. 169-178
[26] Öhman, M., Nordin, A., Bed Agglomeration Characteristics during Fluidized Bed Combustion of Biomass Fuels, *Renewable Energy Resources, 26*(2007), 1, pp. 4550-4559
[27] Wei, B., et al., Investigation of characteristics and formation mechanisms of deposits on different positions in full-scale boiler burning high alkali coal, *Applied Thermal Engineering, 119*(2017), 119, pp. 449-458
[28] Wang, Y., et al., Understanding ash deposition for Zhundong coal combustion in 330 MW utility boiler: Focusing on surface temperature effects, *Fuel, 216*(2018), pp. 697-706
[29] Niu, Y., et al., Further study on biomass ash characteristics at elevated ashing temperatures: The evolution of K, Cl, S and the ash fusion characteristic, *Bioresource Technology, 129*(2013), pp. 642-645
[30] Kassman, H., et al., The importance of SO2 and SO3 for sulphation of gaseous KCl - An experimental investigation in a biomass fired CFB boiler, *Combustion & Flame, 157*(2010), 9, pp. 1649-1657
[31] Chanpirak, A., et al., Sulfation of Gaseous KCl by H2SO4, *Energy & Fuels, 37*(2023), 3, pp. 2319-2328
[32] Zhang, H., et al., Investigation of Ash Deposition Dynamic Process in an Industrial Biomass CFB Boiler Burning High-Alkali and Low-Chlorine Fuel, *RSC advances, 10*(2020), 36, pp. 21420-21426
[33] Enders, M., et al., Temperature-Dependent Fractionation of Particulate Matter and Sulfates from a Hot Flue Gas in Pressurized Pulverized Coal Combustion (PPCC), *Energy & Fuels, 14*(2000), 4, pp. 806-815

Submitted: 28.03.2025

Revised: 21.05.2025

Accepted: 02.06.2025